IEEE Access
Multidisciplinary | Rapid Review | Open Access Journal

Received July 6, 2018, accepted August 14, 2018, date of publication August 17, 2018, date of current version September 7, 2018.

Digital Object Identifier 10.1109/ACCESS.2018.2866060

A High-Precision Wavelength Demodulation Method Based on Optical Fiber Fabry-Perot Tunable Filter

WANSHAN ZHU[1,2,3], JIN WANG[1,2], JUNFENG JIANG[1,2], XINGGANG LIU[3], AND TIEGEN LIU[1,2]

[1]College of Precision Instrument and Optoelectronics Engineering, Tianjin University, Tianjin 300072, China
[2]The Key Laboratory of Optoelectronics Information Technology, Ministry of Education, Tianjin 300072, China
[3]Tian Jin Global Magnetic Card Co., Ltd., Tianjin 300202, China

Corresponding authors: Junfeng Jiang (jiangjfjxu@tju.edu.cn) and Tiegen Liu (tgliu@tju.edu.cn)

This work was supported in part by the National Key Instrument and Equipment Development Projects under Grant 2013YQ030915, in part by the National Natural Science Foundation of China under Grant 61227011, Grant 61378043, Grant 61475114, Grant 61108070, and Grant 11004150, in part by the Tianjin Natural Science Foundation under Grant 13JCYBJC16200, and in part by the Tianjin Science and Technology Support Key Project under Grant 11ZCKFGX01900.

ABSTRACT A high-precision wavelength demodulation method based on optical fiber Fabry–Perot tunable (FPT) filter is proposed for the fiber Bragg grating temperature sensing system. This algorithm uses the original sampling data obtained from the data acquisition card to simultaneously calculate the transmission spectrum of the F-P etalon (FPE) and the reflection spectrum of the fiber Bragg grating (FPG) sensors. In each scanning cycle, the transmission spectrum wavelength of the F-P etalon (FPE) is calibrated dynamically in real time, the reflectance spectrum central wavelength of the FPE sensors is calculated by referring to the transmission spectrum wavelength of the FPE that has been calibrated. It effectively weakens the perturbation effect caused by the nonlinear and non-reproducibility of narrowband light source from the fiber FPT filter, reduces the numerical error and effectively eliminates the pseudo peak of the FPE, and greatly improves the measurement accuracy of the system. Most programming languages can implement this algorithm. A temperature sensing experiment for the proposed method has been carried out. Results showed that the demodulation precision by our method could reach up to ± 0.2 °C, wavelength demodulation accuracy 3 pm.

INDEX TERMS Data acquisition card, demodulation algorithm, fiber Bragg grating, Fabry-Perot, F-P etalon, fiber F-P tunable filter, temperature sensing system.

I. INTRODUCTION

As we all know, fiber Bragg grating (FBG) is one of the fastest growing and most widely used fiber passive components in recent years. FBG sensors belong to the wavelength modulated optical fiber sensor, it can realize the absolute coding of wavelength. When the environmental parameters to be measured change, the wavelength of the FBG will change, which leads to the corresponding change of the central wavelength (or the wavelength of transmission light signal) of the reflected optical signal of the FBG. At the same time, FBG is both a sensing component and a transmission component. FBG has the advantages of light weight, small size, high sensitivity, high resolution, corrosion resistance, high temperature resistance and anti-electromagnetic interference, which is widely used to detect changes in strain, temperature, pressure, magnetic field and so on [1], [2].

Among all FBG detection system, the FBG sensing signal demodulation method is one of the most important technologies of FBG sensor system. Depending on different demodulation principle, there are a variety of demodulation methods for different architectures. Typical signal demodulation methods are as follows: 1) phase unwrapping algorithm [3], this method transforms the FBG wavelength into the corresponding phase; 2) edge filter demodulation [4], [5], [6], this method uses the linear filtering characteristics of some filters to convert the wavelength change of FBG reflected signal into the optical power change, the wavelength demodulation is realized by measuring the

optical power change; 3) matched filter demodulation [7], [8], this method uses similar parameters FBG tracking sensing FBG; 4) tunable Fabry-Perot (F-P) filter demodulation [9], this method uses the wavelength selection characteristic of F-P cavity to realize wavelength demodulation; 5) tunable narrowband laser interrogation method [10], [11], this method uses a tunable narrow band light source to match the reflectance spectrum of the sensing FBG, and other demodulation methods suitable for FBG system [12], [13].

In this paper, we set up a temperature sensor demodulation system based on the fiber F-P tunable filter, and its optical path design is similar to the system demonstrated by Sheng *et al.* [9] in 2015. Compared with the National Instruments (NI) acquisition scheme of the above system, we designed a new data acquisition and demodulation scheme, and proposed a high-precision and effective wavelength demodulation method. Compared with the voltage data of the NI acquisition system, we use the original sampling data obtained from the data acquisition card (DAQ) to simultaneously calculate the transmission spectrum of the F-P etalon (FPE) and the reflection spectrum of the FBG sensor, effectively reducing the numerical error. In each scanning cycle, we first dynamically calibrate the transmission spectrum of FPE in real time, and then calculate the central wavelength of FBG reflectance spectrum by referring to the transmission spectrum of FPE, effectively weakening the perturbation effect caused by the nonlinear and non-reproducibility of narrow light from the fiber F-P tunable filter [9]. We use variance method to eliminate the pseudo peak of FPE. These measures greatly improve the measurement accuracy and speed of the system. In the following sections, we demonstrate in detail the principle of this demodulation method. Most programming languages can implement this algorithm. A temperature experiment for the proposed method has been carried out and the result shows that in the range of 40nm, the data of the FPE and the data of the FBG are relatively stable, the measurement accuracy of ±0.2 °C, wavelength demodulation accuracy 3 pm

II. EXPERIMENTAL SETUP

We set up a temperature sensing experiment system based on the fiber F-P tunable filter, and its optical path design is similar to the system demonstrated by Sheng *et al.* [9] in 2015. We designed a new data acquisition and demodulation scheme. The experiment system consists of a light source unit, a wavelength correction unit, an FBG sensing unit, a data processing unit, and a device driving unit. The light source unit is responsible for improving the effective narrowband light source. The wavelength correction unit is mainly used to calibrate the reflection spectrum of FBG, improve the system measurement accuracy, and increase the system stability. The FBG sensing unit has both sensing unit and transmission unit. In other words, it is both a sensing component and a transmission channel. The data processing unit is mainly responsible for the control of the DAQ, the demodulation of the data, the storage of the data and the display of the data.

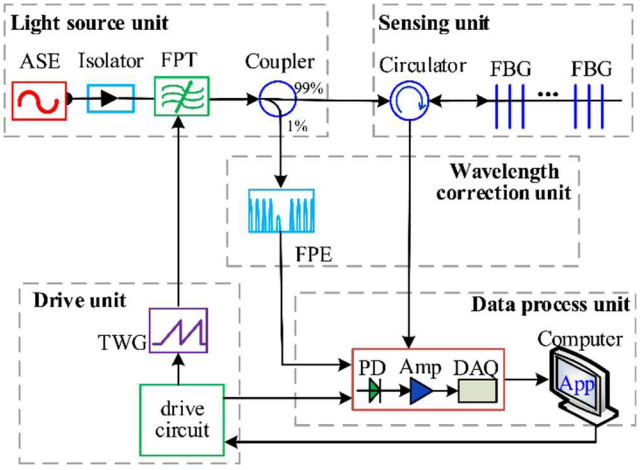

FIGURE 1. Schematic diagram of temperature sensor system based on optical fiber Fabry-Perot tunable filter. ASE = Amplified Spontaneous Emission Light Source; FPT = F-P tunable filter; TWG = triangle wave generator; FPE = F-P etalon; PD = photo diode; Amp = amplifying circuit; DAQ = data acquisition card; App = application program.

The device driver unit is responsible for driving the DAQ and the Triangle Wave Generator (TWG).

As shown in Fig. 1, Amplified Spontaneous Emission Light Source (ASE) protected by fiber isolator emits high power and stable broadband light. The drive circuit controlled by the computer provides a frame synchronization signal to both the TWG and DAQ. The TWG drives the F-P tunable filter (FPT) to produce narrowband light source. Then the narrowband light is coupled into the FPE and FGB sensor according to the 1:99 ratio. The light passing through FPE is called transmission light (FPE_T) and is used for calibration. The light modulated by FBG sensors is reflected to the circulator, we call this reflected light FBG_R. After the FPE_T and the FBG_R pass the DAQ, the digitized signals are sent to the computer via the USB bus, then these data are processed by the application. In view of the openness of our proposed demodulation algorithm, we can use any free programming language to implement it.

In this experiment, the ASE provide broadband light with a range of 1525∼1565 nm, so its measurement range is 40 nm. In each scan cycle, the fiber F-P tunable filter provides 5000 narrowband light of different wavelengths, the spacing between the wavelengths is 8 pm. The 32-channel high-speed DAQ is used in this experiment, its resolution is 16 bit and its sampling rate could reach up to 100 KB/S/Channel.

III. THEORETICAL ANALYSIS

The demodulation schematic diagram of temperature sensing experiment system based on the tunable FP filter is shown in Fig. 2. The schematic illustrates in detail the change in wavelength at each stage of wavelength modulation

Suppose $G(\lambda)$ is represented as the reflection spectrum of FBG, and usually it is assumed as the gaussian distribution,

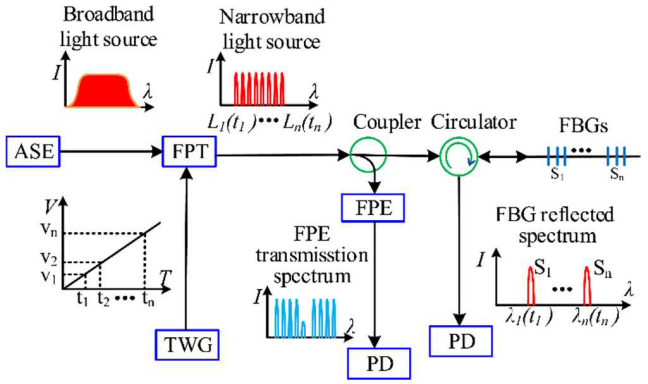

FIGURE 2. Demodulation schematic diagram of temperature sensor system based on optical fiber Fabry-Perot tunable filter. ASE = Amplified Spontaneous Emission Light Source; FPT = F-P tunable filter; TWG = triangle wave generator; FPE = F-P etalon; PD = photo diode.

then there is the following equation:

$$G(\lambda) = I^{(i)} e^{\frac{(\lambda-\lambda_B)^2}{\sigma_0^2}} \tag{1}$$

where $I^{(i)}$ is the incident light intensity of broadband light, λ_B is the reflection wavelength of FBG, σ_0 is the bandwidth of FBG.

The transmission filter function of the F-P tunable filter obtained from Fresnel formula is shown as follows:

$$T_{FP}(\lambda) = \frac{1}{1 + \frac{4R}{(1-R)^2} sin^2\left(\frac{2n\pi cos\varphi \cdot L}{\lambda}\right)} \tag{2}$$

where R is the surface reflectivity of the F-P cavity, n is the refractive index of the medium in the F-P cavity, φ is the incident angle of the transmitted wave to the F-P cavity, L is the length of the F-P cavity, the range of λ is determined by the range of the light source.

The optical power value, $P_D(\lambda)$, received by the photo detector is the correlation integral value of FBG reflectance spectrum and the transmission function of f-p filter, and can be described as:

$$\begin{aligned} P_D(\lambda) &= \int_0^{+\infty} G(\lambda) \cdot T_{FP}(\lambda)\, d\lambda \\ &= \int_0^{+\infty} \frac{(1-R)^2}{(1-R)^2 + 4Rsin^2\left(\frac{2n\pi cos\varphi \cdot L}{\lambda}\right)} I^{(i)} e^{\frac{(\lambda-\lambda_B)^2}{\sigma_0^2}} d\lambda \end{aligned} \tag{3}$$

It is assumed that at *t0* time, λ_B, the reflection wavelength of FBG, meets the transmission maximum condition of the tunable F-P filter. That is to say, when λ_B meets (4), $P_D(\lambda)$ has a maximum value.

$$2(L + \Delta L) = k\lambda_B \tag{4}$$

where ΔL is the cavity length variation of FPT, k is an interference series. Therefore, the reflected wavelength of the sensing FBG can be obtained from the variation value of the cavity length of the FPT.

Next, we will demonstrate the algorithm we mentioned in detail from two aspects, 1) how to calibrate the transmission spectrum of the FPE, 2) how to obtain the central wavelength of the reflection spectrum of sensing FBG.

A. CALIBRATION METHOD OF FPE_T

In order to effectively reduce the perturbation effect caused by the nonlinear and non-reproducibility of narrowband light source from the fiber F-P tunable filter, we dynamically calibrate FPE_T in each FPT scan period.

Firstly, we need to get wave peak numbers of FPE_T, start and end positions of each peak of FPE_T. As shown in Fig. 3, FPE-AD-data is the raw data of FPE_T obtained by the DAQ.

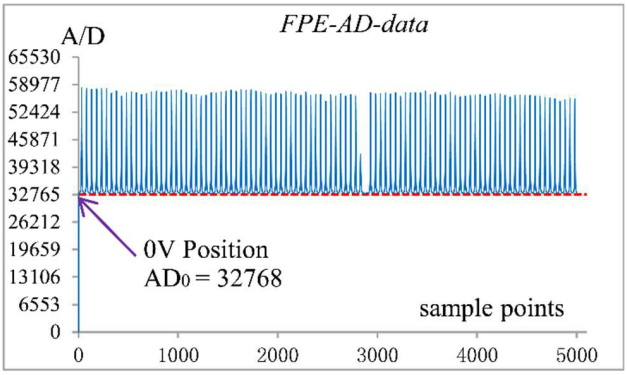

FIGURE 3. Raw AD data of F-P etalon transmission spectrum.

In this experiment, the resolution of DAQ is set to 16 bit and the input voltage is ± 5 *V*. From Fig. 3, AD_0, the value of *0 V*, is 32768, the value of -5 *V* is zero, and the value of $+5$ *V*is 65535. We choose an appropriate parameter to calculate the lower threshold value of FPE_T, and can be described as

$$FPE_{thres} = FPE_{para} \times B_{max} \tag{5}$$

where FPE_{para} is set be *0.25*, B_{max} is the maximum value of B_n.

$$B_n = AD_n - AD_0\,|_{n=1\ldots5000} \tag{6}$$

From (6), the B_n is the different between AD_n and AD_0. As shown in Fig. 4 and Fig. 5, *FPE-Theshold-data* is the spectrum of FPE transmission spectrum after threshold treatment. From Fig. 4, we can see that the value of less than FPE_{thres} is all set to zero. After appropriate threshold processing, noise signal is shielded off. The mapping data of*FPE-Theshold-data* projected onto the X-axis is used to determine M, the weak peak numbers of FPE_T, start and end positions of each peak of FPE_T.

Secondly, we get the position coordinate of the mark in FPE_T, and get rid of the pseudo peak in FPE_T. Equation. (7) is used to determine the position coordinate of central wavelength of FPE_T each peak in the X-axis [14].

$$P_n = \frac{\sum(X_i \times Y_i)}{\sum Y_i} \tag{7}$$

where P_n ($n = 1\ldots M$) is the peaks coordinate in the X-axis, X_i is the horizontal coordinate values of a peak, Y_i is

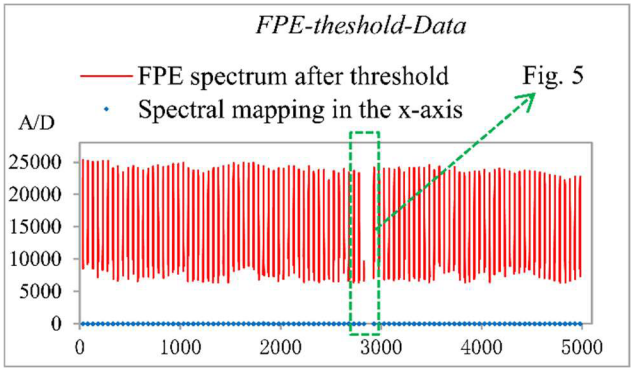

FIGURE 4. Thresholding and mapping of F-P etalon transmission spectrum.

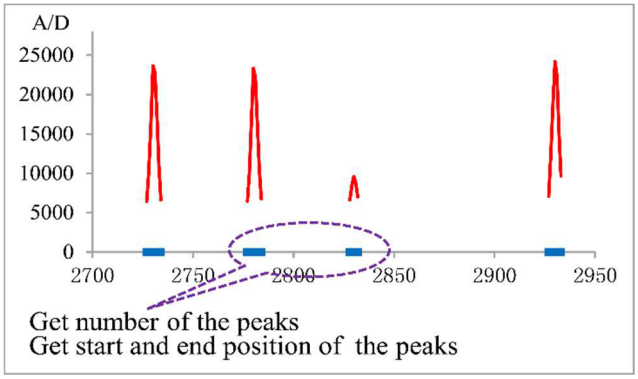

FIGURE 5. Local magnification of Fig. 4

the raw AD sample values of a peak. Then, combined with the (8) and (9), the $PeakP_{avg}$, the average pitch of all peaks, is obtained, where M is peak number.

$$\Delta P_n = P_n - P_{(n-1)}\,|_{n=1\ldots M} \tag{8}$$

$$PeakP_{avg} = \frac{\sum(\Delta P_n)}{M} \times 1.5 \tag{9}$$

Because P_{mark}, the position spacing of the mark in FPE reference profile, is three times as much as the average peak spacing, we get the position coordinate of the mark of FPE_T by $P_{mark} > PeakP_{avg}$. Fig. 6 (a) shows that we get a peak position coordinate in X-axis by (7). Fig. 6 (b) shows that how to get the mark position coordinate of FPE_T by (8) and (9).

In Fig. 6 (b), there is a pseudo peak after the mark. Because the narrowband light source from the F-P tunable filter is very stable, the pseudo peak may be derived from FPE. For this

$$S_n^2 = \left(Y_n - Y_{avg}\right)^2 \tag{10}$$

singular value, (10) is used to remove the pseudo peak of FPE_T, where Y_n $(n = 1\ldots M)$ is the sample value corresponding to P_n rounding, Y_{avg} is the average of Y_n. The pseudo peak position is determined by the maximum variance.

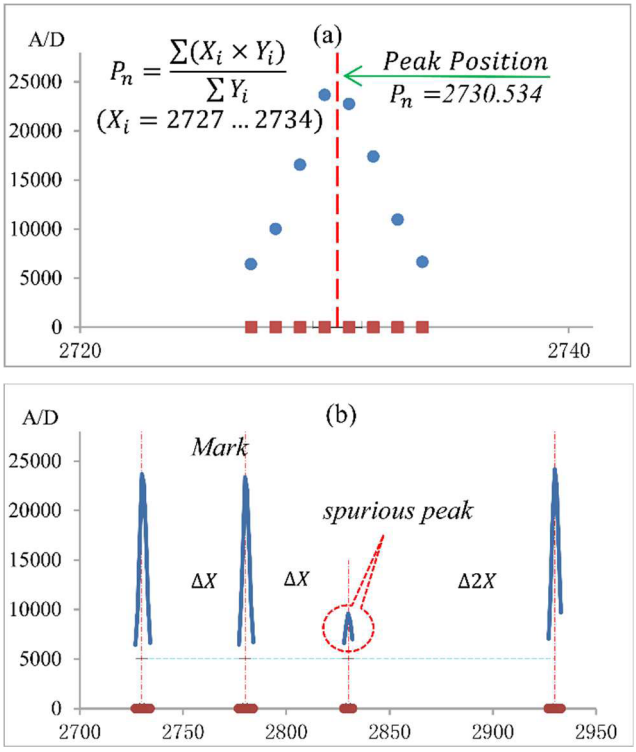

FIGURE 6. (a) Calculate the peak position coordinate in X-axis using the weighted wavelength. (b) Find mark and spurious peak position coordinate.

Thirdly, we complete the calibration of FPE_T with FPE reference profile. From Fig. 7 (a), we can see that the reference wavelength of FPE is not a linear relationship in the strict sense. Therefore, each peak of FPE_T is successively calibrated by the reference wavelength of FPE, then using the linear interpolation method to calibrate the wavelength of each sampling point, the aim is to improve the measurement accuracy. Fig. 7 (b) shows that FPE_T is calibrated by the reference wavelength of FPE, we can see an approximately linear relationship between each peak.

B. GET THE CENTER WAVELENGTH OF FBG_R

In same scan period, we get the center wavelength of the FBG_R. After threshold processing, the noise signal of the FBG_R is removed, we get the peak number of FBG_R, start and end positions of each peak of FBG_R. Equation. (7) is used to get the position coordinate of central wavelength of each peak of FBG_R. Fig. 8 (a) shows that the position coordinate of FBG_R's peak is got by using the above-mentioned method. In Fig. 8 (b), referencing to the calibrated FPE_T data, we use simple geometric function to calculate center wavelength of FBG_R. Finally, the external variables are recovered by polynomial fitting method.

IV. EXPERIMENT RESULTS AND DISCUSSION

We set up a temperature experiment to verify the performance of the method we mentioned. The stability and

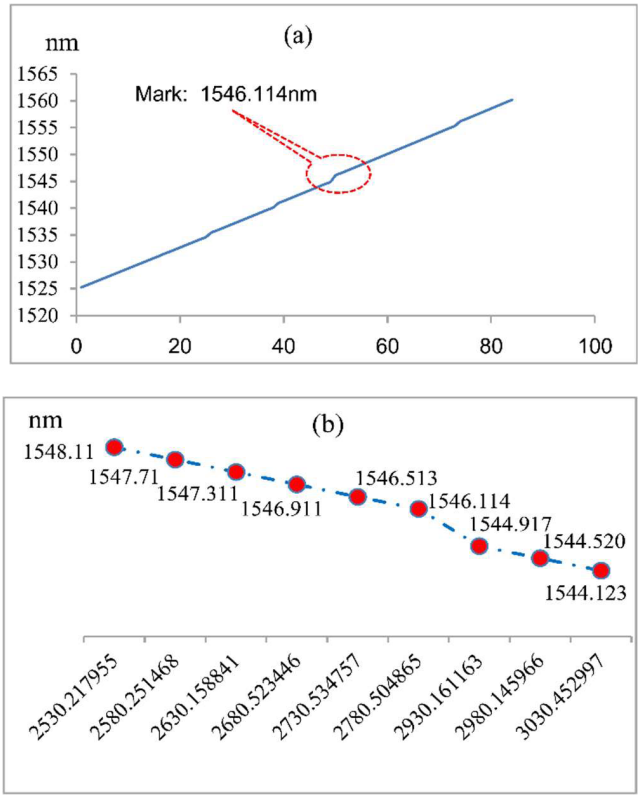

FIGURE 7. (a) F-P etalon reference wavelength. (b) F-P etalon wavelength calibration in each scan period.

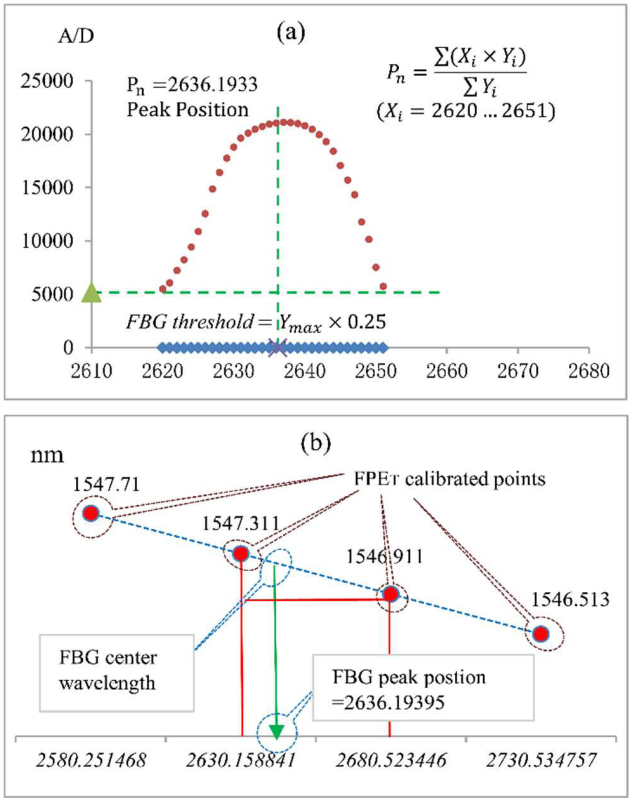

FIGURE 8. FBG_R peak position coordinate in X-axis. (b) Get FBG_R's peak center wavelength by referencing the calibrated F-P etalon wavelength.

accuracy of wavelength demodulation based on tunable F-P filter depend greatly on the relative stability between FPE_T and FBG_R. In this experiment, we selected two FBG sensors with 30 pm/°C temperature sensitivity, and their center wavelength are 1541.191 nm and 1547.263 nm at room temperature. Fig. 9 shows the relationship between temperature and demodulated wavelength when temperature increases from 15 °C to 35 °C at interval 1 °C. From Fig. 9, we can see that the linearity of temperature and wavelength are very good, i.e., this system is very stable. This method effectively weakens the effect of disturbance caused by the nonlinear and non-reproducibility of the narrowband light [15]. Fig. 10 shows the error between demodulated wavelength and wavelength the spectrometer read when temperature increases from 15 °C to 35 °C at interval 1 °C. Here, the resolution of the spectrometer is 60 pm. We can see that there is maximum error of 4 pm in 19 °C, that is to say, system measurement accuracy of ±0.2 °C, wavelength demodulation accuracy 3 pm.

In addition, when calculating the peak position of FPE_T and FBG_R, using different data source will cause some numerical error. Y_{ad} is the raw AD data obtained by DAQ. As shown in (11), Y_v represents the voltage data converted from AD data.$Y_v = \left(\frac{Y_{ad} - AD_{0v}}{AD_{0v}}\right) \times 5$ Equation. (12) shows the numerical error of the peak position by using the AD data

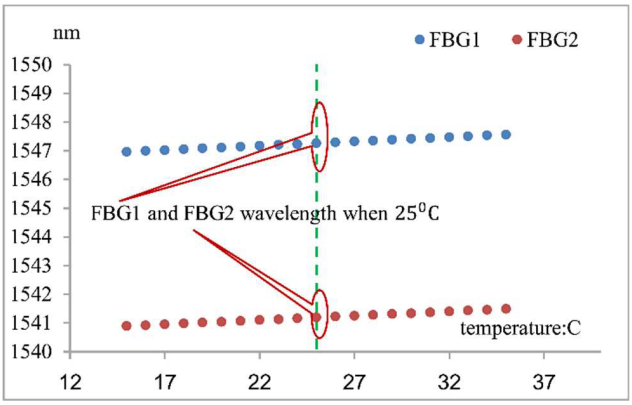

FIGURE 9. Line relationship between demodulation wavelength and temperature.

and the voltage data:

$$Y_v = \left(\frac{Y_{ad} - AD_0}{AD_0}\right) \times 5 \tag{11}$$

$$\begin{aligned} E_n &= \frac{\sum (X_i \times Y_{adi})}{\sum Y_{adi}} - \frac{\sum (X_i \times Y_{vi})}{\sum Y_{vi}} \\ &= \frac{\sum (X_i \times Y_{adi})}{\sum Y_{adi}} - \frac{\sum X_i \times \left(\frac{Y_{adi} - AD_0}{AD_0} \times 5\right)}{\sum \left(\frac{Y_{adi} - AD_0}{AD_0} \times 5\right)} \\ &= \frac{\sum (X_i \times Y_{adi})}{\sum Y_{adi}} - \frac{\sum X_i \times (Y_{adi} - AD_0)}{\sum (Y_{adi} - AD_0)} \end{aligned} \tag{12}$$

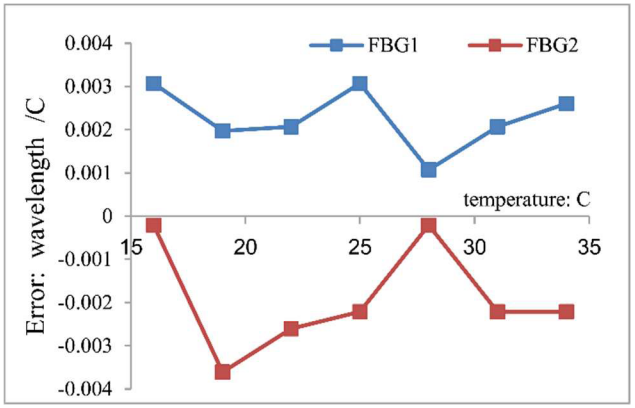

FIGURE 10. Error between demodulation wavelength and wavelength that spectrometer spy.

The more sampling points of each peak are, the greater numerical error E_n is.

V. CONCLUSION

In this letter, a high-precision and effective wavelength demodulation method is proposed. The theory and implementation of this method are analyzed in detail. The temperature experiment based on this method is carried out and the results are analyzed and discussed. The experimental results show that this method is effective and has good performance.

ACKNOWLEDGMENT

I want to take this chance to thanks to my tutors, Dr. Liu Tiegen and Dr. Jiang Junfeng, professors of Tianjin University. In the process of composing this paper, they give me many academic and constructive advices, and help me to correct my paper.

At the same time, I am very grateful of my dear friends, Liu Zhenzhong, Wang Jin, Liu Xinggang, who offered me the confidence and discuss with me about my paper. Of course, I do need to thanks my parent, because of their warm care I can grow up well.

At last, I want to thank my wife and daughter, Wang Cheng and Zhu Mingxi, and I love you!

REFERENCES

[1] P.-C. Peng, H.-Y. Tseng, and S. Chi, "Long-distance FBG sensor system using a linear-cavity fiber Raman laser scheme," *IEEE Photon. Technol. Lett.*, vol. 16, no. 2, pp. 575–577, Feb. 2004.

[2] Y. Tang *et al.*, "Characterization of a fiber Bragg grating (FBG) based palladium tube hydrogen sensor," *Proc. SPIE*, vol. 3670, pp. 532–540, May 1999, doi: 10.1117/12.349766.

[3] Y. Zhu *et al.*, "Temperature insensitive measurements of static displacements using a fiber Bragg grating," *Opt. Express*, vol. 11, pp. 1918–1924, Aug. 2003.

[4] S. M. Melle, K. Liu, and R. M. Measures, "A passive wavelength demodulation system for guided-wave Bragg grating sensors," *IEEE Photon. Technol. Lett.*, vol. 4, no. 5, pp. 516–518, May 1992.

[5] C. J. Misas, F. M. M. Araujo, L. A. Ferreira, J. L. Santos, and J. M. Lopez-Higuera, "Fiber Bragg sensors interrogation based on carrier generation by modulating the coupling length of a wavelength-division multiplexer," *IEEE J. Sel. Topics Quantum Electron.*, vol. 6, no. 5, pp. 750–755, Sep. 2000.

[6] A. Trita *et al.*, "Simultaneous interrogation of multiple fiber Bragg grating sensors using an arrayed waveguide grating filter fabricated in SOI platform," *IEEE Photon. J.*, vol. 7, no. 6, pp. 1–11, Dec. 2015.

[7] A. B. L. Ribeiro, L. A. Ferreira, and J. L. Santos, "Analysis of the reflective-matched fiber Bragg grating sensing interrogation scheme," *Appl. Opt.*, vol. 36, no. 4, pp. 934–939, Feb. 1997.

[8] B.-J. Peng, Y. Zhao, Y. Zhao, and J. Yang, "Tilt sensor with FBG technology and matched FBG demodulating method," *IEEE Sensors J.*, vol. 6, no. 1, pp. 63–66, Feb. 2006.

[9] W. Sheng, G. D. Peng, Y. Liu, and N. Yang, "An optimized strain demodulation method for PZT driven fiber Fabry–Perot tunable filter," *Opt. Commun.*, vol. 349, pp. 31–35, Aug. 2015.

[10] G. A. Ball, W. W. Morey, and P. K. Cheo, "Fiber laser source/analyzer for Bragg grating sensor array interrogation," *J. Lightw. Technol.*, vol. 12, no. 4, pp. 700–703, Apr. 1994.

[11] LS. Yan, A. Yi, W. Pan, and B. Luo, "A simple demodulation method for FBG temperature sensors using a narrow band wavelength tunable DFB laser," *IEEE Photon. Technol. Lett.*, vol. 22, no. 18, pp. 1391–1393, Sep. 2010.

[12] H. Ming, L. Tongqing, H. Lingling, and Z. Qi, "Intensity-demodulated fiber-ring laser sensor system for acoustic emission detection," *Opt. Express*, vol. 21, no. 24, pp. 2976–29269, Dec. 2013.

[13] L. Tongqing, H. Lingling, and H. Ming, "Adaptive ultrasonic sensor using a fiber ring laser with tandem fiber Bragg gratings," *Opt. Lett.*, vol. 39, no. 15, pp. 4462–4465, Aug. 2014.

[14] K. Liu *et al.*, "Investigation of wavelength modulation and wavelength sweep techniques in intracavity fiber laser for gas detection," *J. Lightw. Technol.*, vol. 29, no. 1, pp. 15–21, Jan. 2011.

[15] K. Liu *et al.*, "Investigation of PZT driven tunable optical filter nonlinearity using FBG optical fiber sensing system," *Opt. Commun.*, vol. 281, no. 12, pp. 3286–3290, Feb. 2008.

WANSHAN ZHU received the B.S. degree from the Tianjin University of Technology, China, in 1999, and the M.S. degree from Tianjin University, China, in 2013, where he is currently pursuing the Ph.D. degree in photoelectrons and photonics.

He has been involved in optical fiber sensing technology, photoelectric detection technology, photoelectric integration technology, and embedded image detection technology.

JIN WANG was born in Shenyang, Liaoning, China, in 1985. He received the B.S. degree from Northwestern Polytechnical University, China, in 2008, and the M.S. degree from the China Academy of Telecommunications Technology, China, in 2011. He is currently pursuing the Ph.D. degree in optical engineering with Tianjin University, China.

His research interest includes optical fiber sensing technology, OCT imaging technology, and microwave photonics.

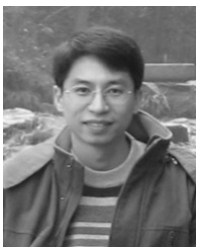

JUNFENG JIANG received the B.S. degree from the Southwest Institute of Technology, China, in 1998, and the M.S. and Ph.D. degrees from Tianjin University, China, in 2001 and 2004, respectively.

He is currently a Professor with Tianjin University. His research interests include fiber sensors and optical communication performance measurement.

XINGGANG LIU received the B.S. degree in electronics from Nankai University, Tianjin, China, in 1990.

He is mainly involved in the development and promotion of products and applications, such as urban digital management, urban intelligent transportation, urban interconnection and communication, and small financial consumption.

TIEGEN LIU received the B.Eng., M.Eng., and Ph.D. degrees from Tianjin University, China, in 1982, 1987, and 1999, respectively.

He is currently a Professor with Tianjin University. His research interests involve photoelectric detection and fiber sensing. He is also a Chief Scientist of the National Basic Research Program of China.